AIP | Journal of Applied Physics

A high power impulse magnetron sputtering model to explain high deposition rate magnetic field configurations

Priya Raman, Justin Weberski, Matthew Cheng, Ivan Shchelkanov, and David N. Ruzic

Citation: Journal of Applied Physics **120**, 163301 (2016); doi: 10.1063/1.4965875
View online: http://dx.doi.org/10.1063/1.4965875
View Table of Contents: http://scitation.aip.org/content/aip/journal/jap/120/16?ver=pdfcov
Published by the AIP Publishing

A high power impulse magnetron sputtering model to explain high deposition rate magnetic field configurations

Priya Raman, Justin Weberski, Matthew Cheng, Ivan Shchelkanov, and David N. Ruzic
University of Illinois at Urbana Champaign, Urbana, Illinois 61801, USA

(Received 21 June 2016; accepted 10 October 2016; published online 24 October 2016)

High Power Impulse Magnetron Sputtering (HiPIMS) is one of the recent developments in the field of magnetron sputtering technology that is capable of producing high performance, high quality thin films. Commercial implementation of HiPIMS technology has been a huge challenge due to its lower deposition rates compared to direct current Magnetron Sputtering. The cylindrically symmetric "TriPack" magnet pack for a 10 cm sputter magnetron that was developed at the Center for Plasma Material Interactions was able to produce higher deposition rates in HiPIMS compared to conventional pack HiPIMS for the same average power. The "TriPack" magnet pack in HiPIMS produces superior substrate uniformity without the need of substrate rotation in addition to producing higher metal ion fraction to the substrate when compared to the conventional pack HiPIMS [Raman *et al.*, Surf. Coat. Technol. **293**, 10 (2016)]. The films that are deposited using the "TriPack" magnet pack have much smaller grains compared to conventional pack DC and HiPIMS films. In this paper, the reasons behind the observed increase in HiPIMS deposition rates from the TriPack magnet pack along with a modified particle flux model is discussed. *Published by AIP Publishing.*
[http://dx.doi.org/10.1063/1.4965875]

I. INTRODUCTION

High Power Impulse Magnetron Sputtering (HiPIMS) is a fairly new ionized Physical Vapor Deposition (iPVD) technique where very short, high power pulses are applied to the target at very low duty cycles so that the average power is the same as that of direct current Magnetron Sputtering (dcMS). These very short high peak power pulses lead to highly dense plasma in front of the target, which ionizes the sputtered material.[2] Higher fraction of ionized sputtered flux to the substrate in HiPIMS leads to high quality films on the substrate. In spite of making high quality films, HiPIMS suffers from lower deposition rates when compared to dcMS due to the huge contribution from the "return effect" of the ionized sputter material.[3,4] The "TriPack" magnet pack[1,5] has already demonstrated increased deposition rates in HiPIMS due to the modification of the magnetic field profile above the target surface. In this work, the microstructure of the deposited film using the "TriPack" was tested and the ion flux to the substrate from the "TriPack" was measured. A modified particle flux model was developed to explain the reasons behind higher deposition rates in "TriPack" based on the HiPIMS particle flux model of Anders.[6]

II. EXPERIMENTAL SET-UP

The magnetic field configuration of the "TriPack" and the conventional magnet pack as well as its experimental set-up is well described in Raman *et al.*[1] Due to manufacturing issues during the "TriPack" magnet pack fabrication, the magnetron targets used with "TriPack" were made to look like pre-eroded targets to increase the magnitude of the magnetic field on the target surface and to simulate a target in the middle of its lifetime. A detailed description of the target modification can be found in Raman *et al.*[1] Further, this specially modified TriPack design from Raman *et al.*[1] will be referred to as TriPack V300 throughout this discussion. Figure 1(a) is the axisymmetric illustration of the modified TriPack V300 target. The colored iso-lines show the total magnitude of magnetic field in Gauss. Figure 1(b) is the top down photograph of the TriPack V300 titanium target and Figure 1(c) shows the pre-eroded titanium target with magnetic insert slots.

III. RESULTS

Figure 2 shows the HiPIMS VI (Voltage-Current) waveform of conventional and TriPack V300 magnet pack with an aluminium target for an average power of ~450 W at 13 mTorr.[1] In order to understand the surface morphology of the films deposited using TriPack V300, copper thin films were deposited on a silicon substrate using the conventional and the TriPack V300 with DC and HiPIMS power supplies at 10 mTorr and 500 W average power. The target to substrate distance in these experiments is 10.2 cm. Figures 3(a), 3(b), and 3(c) shows top down 200k zoom SEM images of copper films deposited using conventional pack DC, conventional HiPIMS, and TriPack V300 HiPIMS respectively.

It is evident from Figure 3(a), that the copper thin film deposited using conventional dcMS consist of highly porous large grains with globular microstructures. In the case of conventional pack HiPIMS (Figure 3(b)), the copper grains are smaller and less porous compared to dcMS deposited copper film, indicating the presence of few copper ions. It is very clear from Figure 3(c) that the copper film deposited using TriPack V300 with HiPIMS consists of very fine globular nanostructure indicating the presence of high ion flux

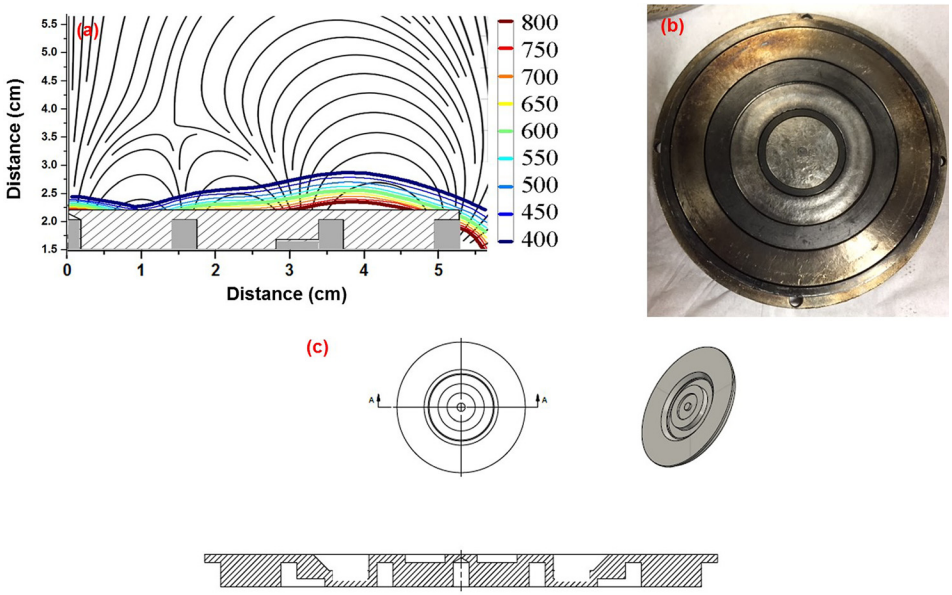

FIG. 1. (a) 2D axisymmetric illustration of the modified TriPack V300 target. The colored iso-lines show the total magnitude of magnetic field in Gauss,[1] (b) Titanium TriPack V300 target with magnetic insets, (c) Pre-eroded target with magnetic inset slots.

with low energies. In all these experiments, the substrate was not biased. Hence, the ion energies of the incoming ion flux were not altered. Increase in ion flux to the substrate causes repeated nucleation that suppresses the columnar structure and transforms the films from a polycrystalline to a globular nanocrystalline microstructure.[7] It can also be observed from the SEM images that the copper film that was deposited using TriPack V300 HiPIMS has lower surface roughness and higher density compared to films deposited using conventional pack DC and HiPIMS.

In order to estimate the metal ion fraction in the deposition flux from the TriPack V300 and conventional pack, two circular stainless steel coupons with known masses were installed side by side. Both the coupons were separated by a ceramic break and a bias cable was attached to one of the coupons so that it is positively biased during deposition to repel the ions. These coupons were mounted on a rotatable feed-through so that the whole experiment can be done without breaking the vacuum. The target material was copper in these experiments and the target to coupon distance was 10.2 cm. A grounded mesh with a transparency of 38% was placed in front of the copper target to avoid the change in plasma potential due to the positive bias on the coupon. Copper films were grown on the stainless steel coupons at +35 V and floating potential. The positive voltage repels all the ions, so the deposition flux on the biased coupon consists of only copper neutrals. The coupon that was at floating potential receives both ion and neutral copper flux. By comparing the relative change in the masses before and after deposition on the two coupons, the ion fraction can be determined.

The results from the ion fraction experiments are shown in Table I and these experiments were performed at 10 mTorr, 500 W average power and 10.2 cm away from the target. The weighing balance that was used to measure the stainless steel coupons can resolve accurately above 1 mg. Therefore, the observed 1 mg change in the biased and unbiased cases of conventional DC and HiPIMS experiments

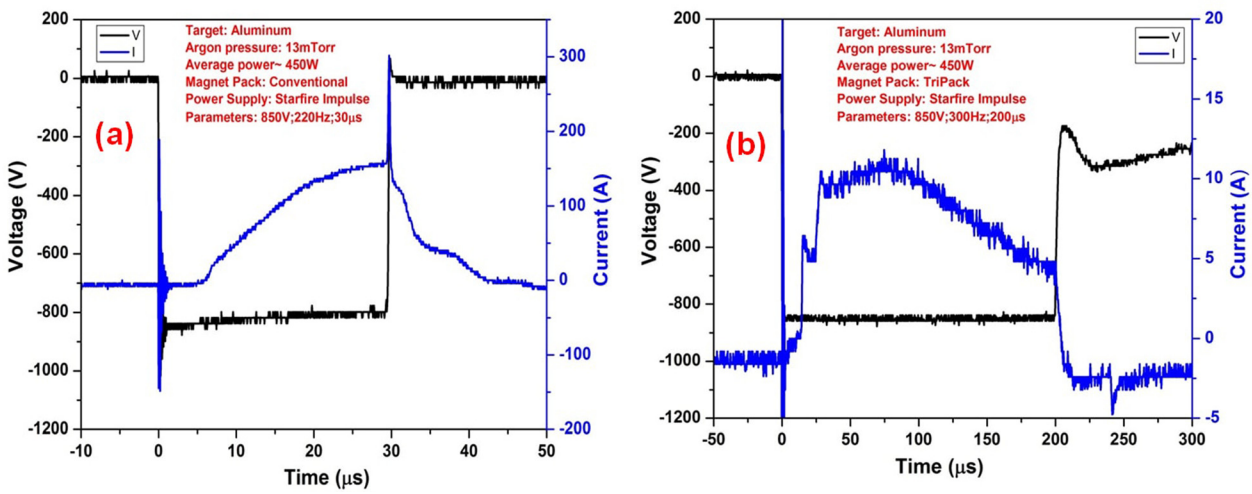

FIG. 2. (a) Voltage and current traces from Starfire Impulse power supply for conventional pack at 13 mTorr, 450 W average power with an aluminum target, (b) Voltage and current traces from Starfire Impulse power supply for TriPack V300 at 13 mTorr and 450 W average power with an aluminum target.[1]

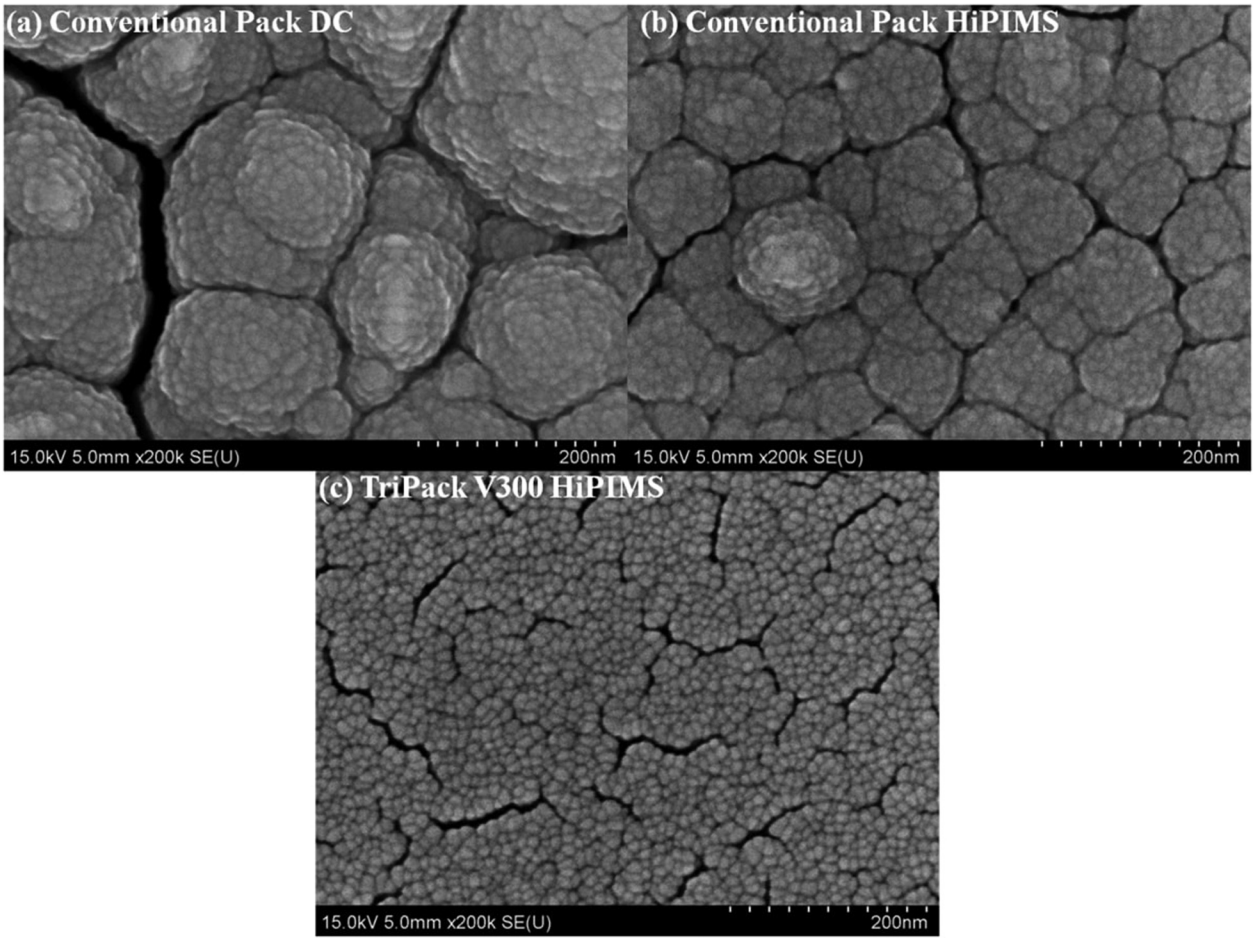

FIG. 3. (a) Top down 200k zoom SEM image of conventional pack copper film deposited with dcMS at 10 mTorr and 500 W average power, (b) Top down 200k zoom SEM image of conventional pack copper film deposited with HiPIMS at 10 mTorr and 500 W average power (c) Top down 200k zoom SEM image of TriPack V300 copper film deposited with HiPIMS at 10 mTorr and 500 W average power.

cannot be used for ion fraction calculations as it is below the accuracy of the weighing balance. This means, the ion fraction in these cases would be less than 5% and the exact number is below the detection limit of this set-up. It can be observed from Table I that in the case of TriPack V300 HiPIMS, the copper ion fraction is ~16% which is almost three times the ion fraction of conventional packs DC and HiPIMS cases.

IV. DISCUSSION

TriPack V300's magnetic field configuration is very different from the conventional pack's magnetic field configuration. The reason behind higher HiPIMS deposition rates in TriPack V300 is therefore related to the difference in the magnetic field configuration which in turn influences the plasma dynamics of the magnet pack. In this section, various features of the magnetic field configurations are analyzed in detail for understanding the influence of the magnetic field configurations on the deposition rates.

TABLE I. Results from copper ion fraction experiments.

Magnet pack	Type of discharge	Average power (W)	Mass change in biased coupon (mg)	Mass change in un-biased coupon (mg)	Ion fraction (%)
Conventional	DC	500	20 ± 1	19 ± 1	$<5 \pm 2$
Conventional	HiPIMS	500	16 ± 1	15 ± 1	$<5 \pm 2$
TriPack V300	HiPIMS	500	16 ± 1	20 ± 1	16 ± 3

A. Magnetic field gradients

The gradient of the magnetic field component that is parallel to the surface of the target (radial magnetic field B_r) is an important factor in determining the plasma parameters in front of the target surface. For better understanding, the gradient (along "z" direction) of radial magnetic fields on three different locations (Figures 4(a) and 4(b)) on the top of the conventional pack and TriPack V300 target surfaces are plotted against the distance from the target surface (Figures 4(c) and 4(d)). TriPack V300 consists of three race tracks, where the inner and outer racetracks have radial fields directed (red color) in the opposite direction to the middle race track (blue color). In the case of the TriPack V300, location 1 corresponds to the inner race track, location 2 corresponds to the middle race track, and location 3 corresponds to the outer race track.

It can be observed from Figure 4(c) that the conventional magnet pack has radial magnetic field gradients of few hundred Gauss/cm in the region above the target. Although the gradients are low in the region (location 2) above the race

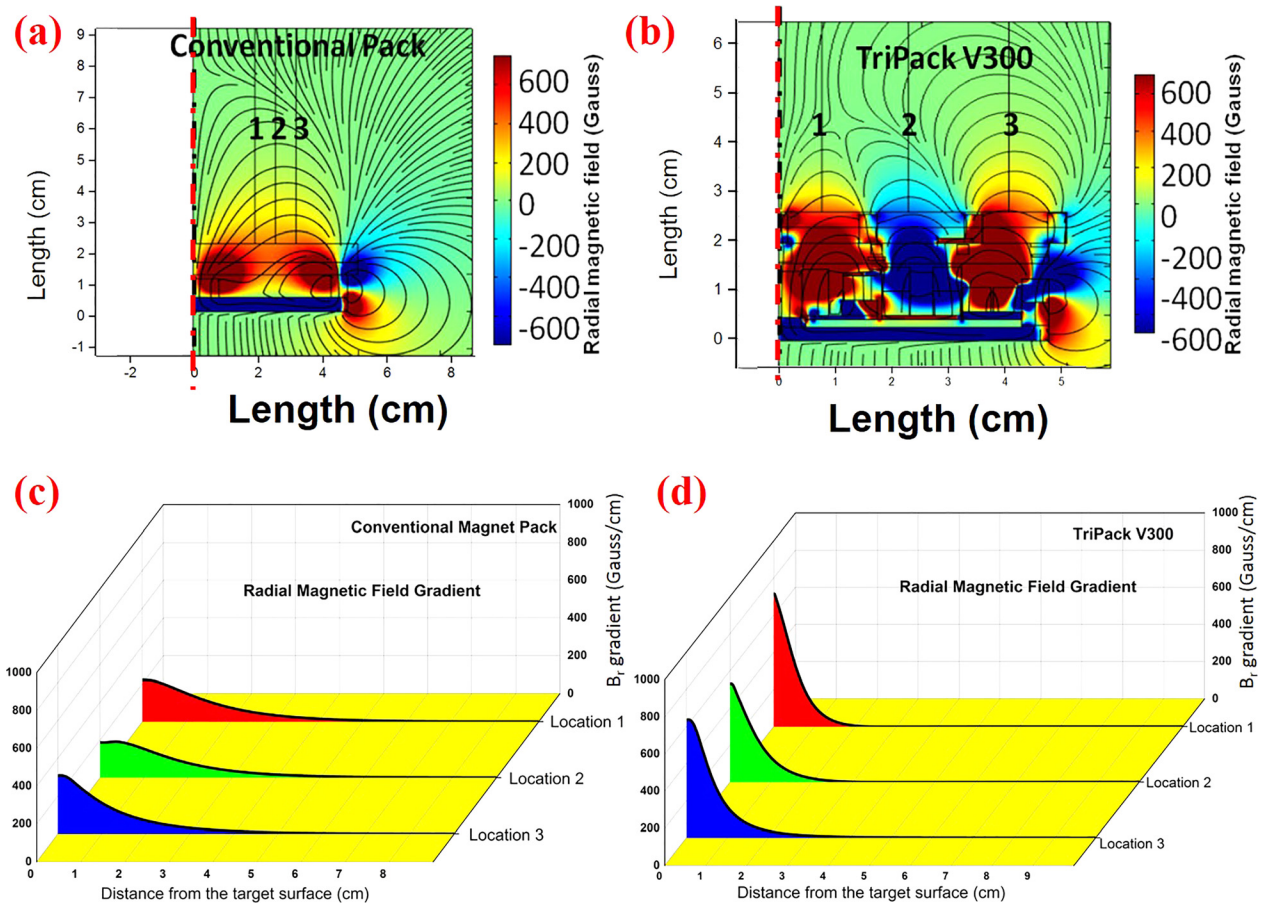

FIG. 4. (a) Magnitude of the radial magnetic field distribution above 0.635 cm target surface in the conventional magnet pack with Br and Bz components, Color legend is in Gauss. Numbered lines correspond to locations in (c). Since this magnet pack is cylindrically symmetric, 2D axisymmetric simulation results are presented, (b) Magnitude of the radial magnetic field distribution 0.635 cm above the target surface in the TriPack V300 magnet pack with Br and Bz components, Color legend is in Gauss. Since this magnet pack is cylindrically symmetric, 2D axisymmetric simulation results are presented. Numbered lines correspond to locations in (d). (c) Gradient of radial magnetic field at various distances from the conventional target surface on the three locations corresponding to (a). (b) Gradient of radial magnetic field at various distances from the conventional target surface on the three locations corresponding to (b).

track, the magnitude of the radial magnetic field is ~430 G. Whereas in the case of TriPack V300, the radial magnetic field gradients from all the three race tracks in TriPack V300 are much higher and falls sharply (Figure 4(d)) compared to the gradients from the conventional pack (Figure 4(c)).

B. Diffusion across the magnetic field

The Debye length and sheath thickness for TriPack V300 and conventional pack HiPIMS plasma can be calculated from Equations (1) and (2).

$$\lambda_D = \sqrt{\frac{\varepsilon_0 k T_e}{n_e e^2}}, \tag{1}$$

$$S_{child} = \frac{\sqrt{2}}{3}\lambda_D \left(\frac{2eV_0}{KT_e}\right)^{\frac{3}{4}}, \tag{2}$$

where T_e is the electron temperature and V_0 is the discharge voltage. The Child sheath formula cannot be applied in the case of HiPIMS due to the presence of magnetic field and non-Maxwellian electrons but can be used for order of magnitude estimate.[8] For an electron temperature of 5 eV and discharge voltage of 600 V, the Debye length is $\sim 5.2 \times 10^{-4}$ cm, and the sheath thickness is roughly estimated to be ~0.1 cm. Therefore, the pre-sheath thickness can be assumed to be ~1–2 cm. By taking into account the acceleration of ions in the pre-sheath, ion energy is roughly assumed to be ~2.5 eV. The working pressure for both magnet packs is 10 mTorr. Hence, the neutral density can be estimated from Equation (3).[9]

$$n_n = 3.13 \times 10^{13} p(\text{mTorr}) \text{cm}^{-3} . \tag{3}$$

For the working gas pressure of 10mTorr, $n_n = 3.3 \times 10^{14}$ cm^{-3}. During the HiPIMS process, the sputtered atoms collide with the working gas, which leads to heating and expansion of the working gas. This effect is known as gas rarefaction and the background gas temperature increases from ~300 K to 600 K during this process in the HiPIMS discharge.[10] At 600 K and 10 mTorr, the neutral density is estimated to be $\sim n_n = 1.65 \times 10^{14}$ cm^{-3}.

Particles (electrons and ions) can move across the magnetic field along the gradients when there are collisions. For this analysis, the pre-sheath region is considered. In order to roughly estimate the diffusion co-efficient across the magnetic fields, the following assumptions are made:

1. The working pressure for both packs is 10 mTorr.
2. The neutral density taking into account the gas rarefaction process is $n_n = 1.65 \times 10^{14}\,cm^{-3}$.
3. The collision frequency is driven by ion-neutral, electron-neutral, ion-ion, electron-electron, and electron-ion collisions. The electron density (n_e) measured from the Triple Langmuir Probe (TLP) experiments is $\sim 10^{13}\,cm^{-3}$ and the neutral gas density is $1.65 \times 10^{14}\,cm^{-3}$ at ~ 7.6 cm away from the target surface, which means that the largest contributing collision process will be electron-neutral and ion-neutral collision and they will dominate the diffusion co-efficient. Hence, only these two processes will be considered in diffusion co-efficient calculations.
4. The electron energy is assumed to be 5 eV (TLP measurements) and the energy of the ions is assumed to be ~ 2.5 eV taking into account the acceleration in the plasma pre-sheath.

The diffusion co-efficient across the magnetic field is calculated from Equation (4).[11]

$$D_{perp} = \frac{r_L^2}{\tau}. \tag{4}$$

Here, r_L^2 is the Larmor radius and τ is the mean time between collisions. The Larmor radius can be calculated from Equation (5).

$$r_L = \frac{mv}{Bq}, \tag{5}$$

$$\tau^{-1} = n_n \sigma v, \tag{6}$$

$$D_{perp} = \frac{\lambda v_{avg}}{2}, \tag{7}$$

$$\lambda = \frac{0.061\,\text{m}}{p[\text{mTorr}]} \tag{8}$$

where m is the mass of the particle, ν is the velocity component perpendicular to the direction of magnetic field, B is the magnetic field, q is the electronic charge, σ is the collision cross-section, λ is the mean free path,[12] and ν_{avg} is the average speed. If the magnetic field $B \to 0$, then $r_L \to \infty$. When $r_L \geq \lambda$ (mean free path), the diffusion is no longer controlled by the magnetic field; therefore, the formula for diffusion co-efficient across the magnetic field becomes

$$D_{perp} = \frac{\lambda^2}{\tau}. \tag{9}$$

From the above equations, the electron diffusion across the magnetic field due to electron-neutral (electron-argon) collision process is calculated along the three locations shown in Figures 4(a) and 4(b) for the conventional and the TriPack V300 magnet packs.

Since the location of the middle race track of the TriPack V300 and location 2 of the conventional magnet pack approximately correspond on the target surface, their electron D_{perp} across the magnetic field are compared in Figure 5. It can be seen from Figure 5, that D_{perp} in the middle race track of TriPack V300 increases much more steeply

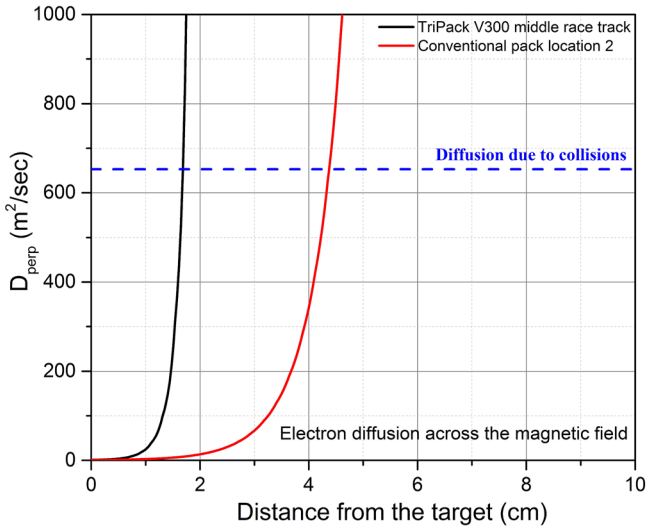

FIG. 5. Comparison of electron diffusion co-efficient across the magnetic field from conventional pack location 2 and TriPack V300 middle race track. The dashed blue line is from diffusion due to collisions, so after 1.8 cm from the TriPack V300, the magnetic field has little effect. That same number for the conventional pack is 4.3 cm.

and reaches a value of 652.8 m^2/s (diffusion co-efficient when $r_L = \lambda$) at 1.5 cm from the target surface, whereas the conventional pack reaches the same value only at 4.3 cm from the target surface. This clearly indicates that the plasma diffuses more quickly along the steep magnetic field in the TriPack V300. The dashed line in Figure 5 is the diffusion coefficient due to collisions with the background gas. At ~ 1.8 cm away, the magnetic field has little effect on the electrons in the TriPack V300 while in the standard pack the magnetic field still confines the electrons up to a height of 4.3 cm.

The ambipolar diffusion co-efficient across the magnetic field can be calculated from the following equation:[13]

$$D_{ambi} = \frac{2D_{perp}^{ions} D_{perp}^{elect}}{\left(D_{perp}^{ions} + D_{perp}^{elect}\right)}, \tag{10}$$

D_{perp}^{elect} is the diffusion co-efficient of electrons across the magnetic field and D_{perp}^{ions} is the diffusion co-efficient of ions across the magnetic field which can be calculated from Equation (9). For calculating D_{perp}^{ions}, ion-neutral (argon ion-argon) cross section was used.

Figure 6(a) is the comparison plot of the ambipolar diffusion co-efficient (D_{ambi}) versus distance from the target surface along location 2 of conventional pack and middle race track of TriPack V300. At around 1.3 cm from the target surface, D_{ambi} on the conventional magnet pack (location 2) is 3.3 m^2/s and the D_{ambi} on the middle race track of TriPack V300 is 5.5 m^2/s. This means the ambipolar diffusion co-efficient in the case of TriPack V300 middle race track is 1.6 times more than the conventional magnet pack location 2 at 1.3 cm from the target surface. This clearly points to much higher plasma diffusion from TriPack V300 compared to the conventional pack. Figure 6(b) shows the average plasma diffusion speed for TriPack V300 and conventional magnet pack calculated from Equation (7). It is evident from this

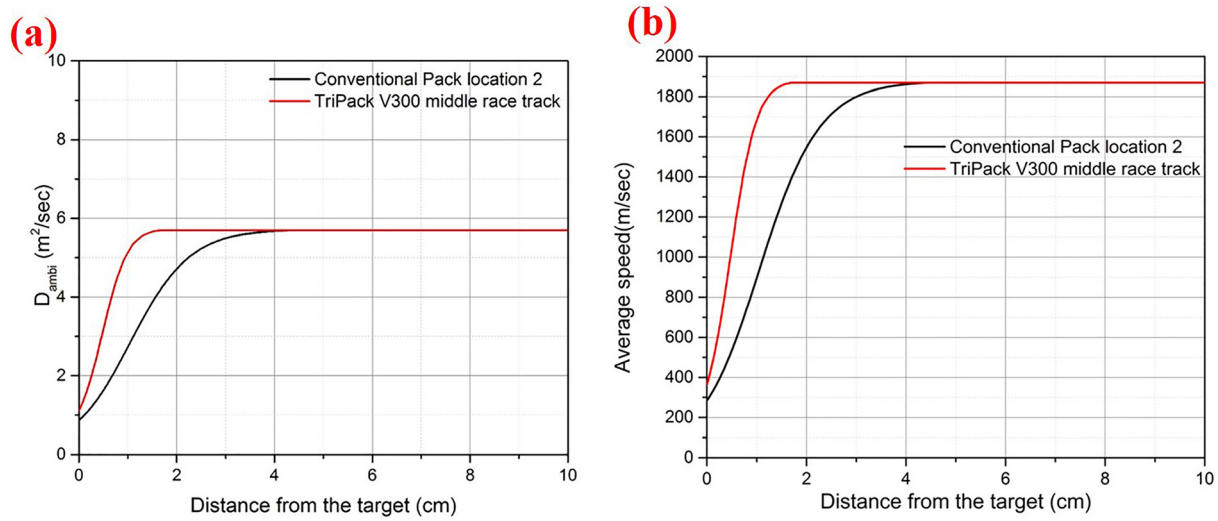

FIG. 6. (a) Comparison of ambipolar diffusion co-efficient from conventional pack location 2 and TriPack V300 middle race track. (b) Comparison of average plasma diffusion speed from conventional pack location 2 and TriPack V300 middle race track.

plot that the average plasma diffusion speed of the conventional pack is only ~60% of TriPack V300 at 1.3 cm from the target surface and the enhanced diffusion allows more plasma to escape the highly confined region.

V. HiPIMS PARTICLE FLUX TRANSPORT MODEL

The particle flux model by Anders[6] takes into account the fluxes involved in the deposition by HiPIMS technique under conditions when the plasma is dominated by metal sputtered from the target (Figure 7(a)). In Figure 7(a), α is the ionization probability in the plasma, β is the probability of ions to return to the target, and γ is the sputter yield. The values of α and β depend on the target material, HiPIMS system and discharge parameters.

Based on Figure 6(a), α and β can be calculated from the following equations:[6]

$$\phi_{a,sub} = (1-\alpha)\phi_{a,\,sputtered}, \tag{11}$$

$$\phi_{i,sub} = \alpha(1-\beta)\phi_{a,\,sputtered}, \tag{12}$$

where $\phi_{a,sub}$ is the atom flux to the substrate, $\phi_{i,sub}$ is the ion flux to the substrate, and $\phi_{a,\,sputtered}$ is the atom flux from the target. For the conventional magnet pack with an aluminum target, α and β can be calculated based on the deposition rates and discharge current during 10 mTorr HiPIMS operation. According to Schmidt *et al.*,[14] in the first few microseconds from the start of the HiPIMS pulse, the discharge is more like DCMS and then it transitions into HiPIMS. Therefore, in these calculations, the average current during the HiPIMS portion of the pulse is used rather than the average current during the entire pulse. The average discharge current in the case of conventional pack is 115 A (Figure 2); therefore, 7.2×10^{20} ions/s reach the target. By multiplying the sputter yield (1.267) corresponding to the discharge voltage of 850 V with the number of ions/s, the number of atoms/s that comes out of the target can be estimated. In the conventional magnet pack case, 9.1×10^{20} atoms/s comes out of the target. The conventional pack erosion area is calculated to be ~38.70 cm^2. Therefore, the target neutral flux $\phi^{con}_{a,\,sputtered}$ is 2.4×10^{19} atoms/cm^2 s. The peak discharge current value is used to calculate the target neutral flux because it influences the deposition rate via α and β.[15] Therefore, peak current values were used instead of the average current in these calculations. The measured aluminum

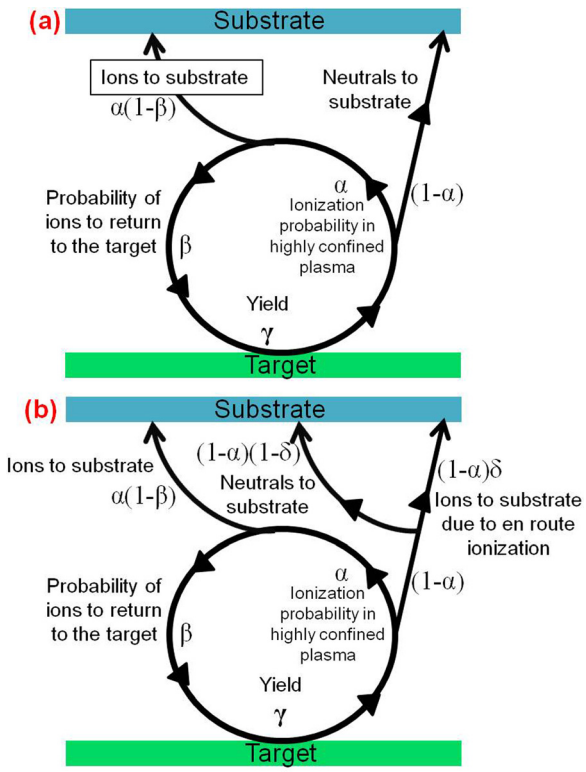

FIG. 7. (a) Schematic representation of the fluxes involved in HiPIMS under conditions when the plasma is dominated by metal sputtered from the target. α represents the ionization probability, β represents the return probability and γ represents the sputter yield.[6] (b) Schematic representation of the fluxes involved in the modified HiPIMS model where α represents the ionization probability in the highly confined plasma, β represents the return probability, γ represents the sputter yield, δ represents the probability of neutrals ionized en route to the substrate.

deposition rate at the substrate for 500 W HiPIMS average power is 6 Å/s. Based on the deposition rate and density of aluminum, the total flux at the substrate is calculated to be 3.6×10^{15} atoms/cm^2 s. From ion fraction experiments, the ion flux to the substrate in the case of conventional pack is ~2%. Therefore, the ion flux to the substrate $\phi^{con}_{i,sub}$ is 7.2×10^{13} atoms/cm^2 s. The α and β values can be calculated from the following equations which takes the geometric solid angle Ω into account.

$$\phi^{con}_{a,sub} = (1-\alpha)\phi^{con}_{a,sputtered}\Omega, \tag{13}$$

$$\phi^{con}_{i,sub} = \alpha(1-\beta)\phi^{con}_{a,sputtered}\Omega. \tag{14}$$

The geometric solid angle calculated based on the quartz crystal microbalance (QCM) area and the throw distance is 8×10^{-4} rad. The neutral flux to the substrate $\phi^{con}_{a,sub}$ is 3.5×10^{15} atoms/cm^2 s. Therefore, $\alpha = 0.818$ and $\beta = 0.995$.

In the case of TriPack V300, the average current is 10 A (Figure 2); therefore, 6.2×10^{19} ions/s reach the target. Based on sputter yield and number of ions/s, 7.9×10^{19} atoms/s comes out of the target. The TriPack V300 erosion area is ~51.61 cm^2. Therefore, the target neutral flux $\phi^{tri}_{a,sputtered}$ is 1.5×10^{18} atoms/cm^2 s. The measured aluminum deposition rate at the substrate for 500 W HiPIMS average power is 9 Å/s. Therefore, the total flux at the substrate is 5.4×10^{15} atoms/cm^2 s. From ion fraction experiments, the ion flux to the substrate in the case of TriPack V300 is ~16%. Therefore, the ion flux to the substrate $\phi^{tri}_{i,sub}$ is 8.6×10^{14} atoms/cm^2 s. The α and β values are calculated from the following equations taking the geometric solid angle into account.

$$\phi^{tri}_{a,sub} = (1-\alpha)\phi^{tri}_{a,sputtered}\Omega, \tag{15}$$

$$\phi^{tri}_{i,sub} = \alpha(1-\beta)\phi^{tri}_{a,sputtered}\Omega. \tag{16}$$

Using the same geometric solid angle of 8×10^{-4} rad and the neutral flux to the substrate $\phi^{tri}_{a,sub} = 4.5 \times 10^{15}$ atoms/cm^2 s, the ionization probability α is calculated to be a negative number −2.75. This means the flux model proposed by Anders.[6] does not work in case of TriPack V300 because $0 \le \alpha \le 1$ condition is not satisfied, and therefore, this model cannot explain the results seen.

Since the magnetic field profile of TriPack V300 is very different from the conventional pack, a modified flux model as shown in Figure 7(b) has to be used. In Figure 7(b), δ is the fraction of neutral atoms that are ionized en route to the target by the expanding plasma. $(1-\alpha)$ corresponds to the neutrals that are not ionized by the highly confined plasma, $(1-\alpha)*(1-\delta)$ corresponds to the actual neutrals reaching the substrate. Based on this modified flux model, α, β and δ can be calculated from the following equations:

$$\phi^{tri}_{a,sub} = (1-\alpha)(1-\delta)\phi^{tri}_{a,sputtered}\Omega P, \tag{17}$$

$$\phi^{tri}_{i,sub} = [\alpha(1-\beta) + \delta(1-\alpha)]\phi^{tri}_{a,sputtered}\Omega P, \tag{18}$$

where Ω is the geometrical solid angle and P is the peaking factor for flux from TriPack V300. The peaking factor takes into account the non-uniform flux distribution from this pack. It has been shown that in HiPIMS, the plasma expansion is associated with a high plasma density peak moving from the target towards the substrate with the magnetic field strength controlling the downstream plasma distribution.[16] The "Spiral" magnet pack described in Yu *et al.*[17] showed a flattened downstream plasma density distribution in HiPIMS. Also, TLP measurements on "Spiral" magnetic field pattern demonstrated more uniform downstream plasma density compared to the other magnetic field patterns tested in that work. In the case of TriPack V300, the measured ion fraction at the substrate ~16% and these ionizations occur away from the highly confined plasma. This leads to non-uniform flux distribution in the case of TriPack V300 since some of the ionizations may be made right in front of the substrate and this makes the peaking factor term necessary in this case. This is explained in detail later in this work.

Both conventional and TriPack V300 magnet packs were operated at 10 mTorr. So, the mean free path is ~0.6 cm and the target to substrate distance is ~10 cm, which means there are a lot of scattering events that would lead to uniform flux distribution at the substrate. Therefore, the peaking factor term is not needed in fitting the conventional pack measurements to Anders model.[6] The peaking factor term in the case of conventional magnet pack is 1. The value of P for TriPack V300 can be estimated from the following equation:

$$P \le \frac{\phi^{tri}_{total,sub}}{\phi^{tri}_{a,sputtered} * \Omega}. \tag{19}$$

Based on Equation (19), the peaking factor for TriPack V300 is estimated to be $P \le 4.5$. In Equation (19), $\phi^{tri}_{total,sub}$ is the total flux arriving at the substrate and $\phi^{tri}_{a,sputtered}$ is the total neutral flux sputtered from the target in the TriPack V300 case.

By substituting the values of $\phi^{tri}_{a,sub}$, $\phi^{tri}_{i,sub}$, $\phi^{tri}_{a,sputtered}$, Ω in Equations (17) and (18), the following equations are obtained:

$$3.75 = (1-\alpha)(1-\delta)P\,, \tag{20}$$

$$0.71 = [\alpha(1-\beta) + \delta(1-\alpha)]P\,. \tag{21}$$

Based on the diffusion speed comparison of both magnet packs, average plasma diffusion speed of TriPack V300 is 1.6 times the average plasma diffusion speed of conventional magnet pack. Hence, we assume that

$$(1-\beta_{tri}) = 1.6(1-\beta_{con}). \tag{22}$$

From Equation (22), $\beta_{tri} = .992$. By dividing Equation (20) by Equation (21), δ is calculated to be 0.159. Substituting $\delta = 0.159$ in Equation (20), the following equation is obtained:

$$4.4 = (1-\alpha)P\,. \tag{23}$$

By substituting $P_{max} = 4.5$ in Equation (23), α is found to be 0.022. Table II shows flux parameter comparison of TriPack V300 and conventional pack.

TABLE II. Flux parameter comparison of conventional and TriPack V300.

Parameter	TriPack V300	Conventional pack
α	0.022 ± 0.007	0.818 ± 0.081
β	$0.992 + 0.008/-0.198$	$0.995 + 0.005/-0.199$
δ	0.159 ± 0.032	0

In the case of the conventional magnet pack, $\alpha = 0.818$, which means that the ionization in the highly confined plasma region is very high. Almost all the ions that are generated in this highly confined plasma region come back to the target because of its high β (0.995) value and this is also evident from the ~2% ion fraction measured at the substrate. Since all the ions return back to the target, $\delta = 0$ in this case. The high value of the average discharge current (115 A) is due to the huge contribution from the metal ion return effect and higher ionization probability in the highly confined plasma region.

In the case of TriPack V300, $\beta = 0.992$ which means all the ions that are produced in the narrow highly confined plasma region (Figure 8) come back to the target. The low value of α indicates lower ionization in the highly confined plasma region, which is evident from the low average discharge current (10 A) measured in this case. The TriPack V300 is operating in the HiPIMS mode as the measured electron density in this case is $\sim 5 \times 10^{12}\,\mathrm{cm}^{-3}$ (Ref. 18) at 7.6 cm away from the target, which is a prominent feature of HiPIMS discharges. Table III shows the peak current densities of conventional magnet pack and TriPack V300 during HiPIMS and DC operation. It can be seen from the Table III that the peak current density of TriPack V300 in HiPIMS is about 9× the current density during DC operation. The optical emission spectroscopy analysis indicated that the conventional pack in HiPIMS discharge contained more aluminum than argon when compared to DC operation. In the case of TriPack V300, the relative intensities of aluminum peak at 397 nm compared to the argon peaks from 650–900 nm in HiPIMS compared to DC indicated pure metal conditions.[18] All these results, clearly points towards TriPack V300 operating in HiPIMS mode.

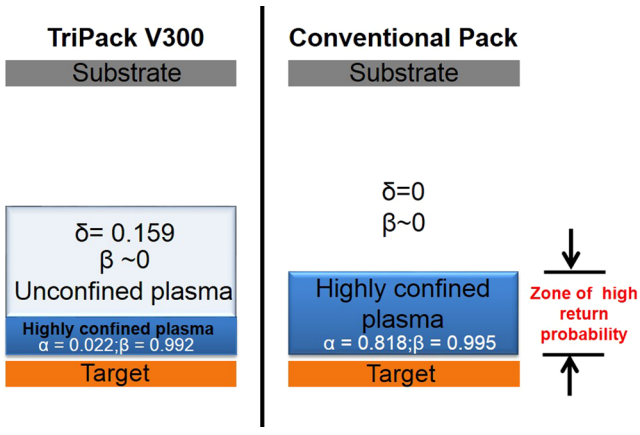

FIG. 8. Representation of flux parameters (α, β and δ) in TriPack V300 and conventional pack in HiPIMS.

TABLE III. Peak current density comparison of conventional and TriPack V300.

Discharge	Conventional pack current density (A/cm^2)	TriPack V300 current density (A/cm^2)
DC	0.03	
HiPIMS	3.88	0.23

The unconfined plasma region in the case of TriPack V300 extends farther and this region helps to ionize the neutrals from the target en route to the substrate leading to higher ion flux at the substrate. The value of δ (probability of neutrals that are ionized in the unconfined plasma region) was calculated to be 0.159 ± 0.032. Some of the neutrals from the target are ionized in the unconfined plasma region of the TriPack V300 and reach the substrate and this is evident from the 16% ion fraction measured at the substrate. It should be noted that the above calculations as well as the modified model are universal regardless of the target material. The main input parameters used in this model are cathode voltage, discharge current, deposition rate, electron density, electron temperature, and ionization fraction. All these values were experimentally measured and entered into the model. Also, based on our ionization fraction measurements, the copper and aluminum ionization fractions were very similar; therefore, the copper ionization fractions values were used in the model. This does not have any significant impact on the updated HiPIMS model and calculations.

VI. CONCLUSION

The fundamental reason behind observed higher HiPIMS deposition rates in the TriPack V300 magnet pack is due to plasma dynamics arising from its unique magnetic field configuration. A modified particle flux transport model was developed to explain the increase in TriPack V300's HiPIMS deposition rates. The films that were deposited using the TriPack V300 magnet pack had much smaller grains compared to conventional pack DC and HiPIMS films. Additionally, TriPack V300 magnet pack generates higher fraction of ionized sputtered material at the substrate compared to the conventional magnet pack.

ACKNOWLEDGMENTS

This research was funded by the NSF Center for Lasers and Plasmas for Advanced Manufacturing under the I/UCRC program Grant No. 15-40030. This work was carried out in part in the Frederick Seitz Materials Research Laboratory Central Research Facilities and Visualization Laboratory at Beckman Institute in University of Illinois.

[1]P. Raman, I. Shchelkanov, J. McLain, M. Cheng, D. Ruzic, I. Haehnlein, B. Jurczyk, R. Stubbers, and S. Armstrong, Surf. Coat. Technol. **293**, 10 (2016).
[2]G. Greczynski and L. Hultman, Vacuum **84**, 1159 (2010).
[3]F. Papa, H. Gerdes, R. Bandorf, A. Ehiasarian, I. Kolev, G. Braeuer, R. Tietema, and T. Krug, Thin Solid Films **520**, 1559 (2011).

[4]P. Raman, I. A. Shchelkanov, J. McLain, and D. N. Ruzic, J. Vac. Sci. Technol. A **33**, 031304 (2015).
[5]D. N. Ruzic, I. A. Shchelkanov, and P. Raman, U.S. patent 20,160,104,607 (2016).
[6]A. Anders, J. Vac. Sci. Technol. A **28**, 783 (2010).
[7]D. Lundin and K. Sarakinos, J. Mater. Res. **27**, 780 (2012).
[8]A. Rauch, R. J. Mendelsberg, J. M. Sanders, and A. Anders, J. Appl. Phys. **111**, 083302 (2012).
[9]F. F. Chen and J. P. Chang, *Lecture Notes on Principles of Plasma Processing* (Springer Science & Business Media, 2012).
[10]N. Britun, M. Palmucci, S. Konstantinidis, and R. Snyders, "Towards deeper understanding of a HiPIMS discharge by time-resolved optical plasma diagnostics," in 13th International Conference on Plasma Surface Engineering, Garmisch-Partenkirchen, Germany (2012).
[11]F. C. Francis, *Introduction to Plasma Physics and Controlled Fusion*, 2nd ed. (Plenum Press, New York and London, 1984).
[12]D. N. Ruzic, *Electric Probes for Low Temperature Plasmas* (American Vacuum Society, 1994).
[13]A. Simon, Phys. Rev. **98**, 317 (1955).
[14]S. Schmidt, Z. Czigány, G. Greczynski, J. Jensen, and L. Hultman, J. Appl. Phys. **112**, 013305 (2012).
[15]V. Tiron, I. Velicu, O. Vasilovici, and G. Popa, J. Phys. D: Appl. Phys. **48**, 495204 (2015).
[16]L. Meng, H. Yu, M. M. Szott, J. T. McLain, and D. N. Ruzic, J. Appl. Phys. **115**, 223301 (2014).
[17]H. Yu, L. Meng, M. M. Szott, J. T. McLain, T. S. Cho, and D. N. Ruzic, Plasma Sources Sci. Technol. **22**, 045012 (2013).
[18]P. Raman, Ph.D. dissertation (University of Illinois at Urbana-Champaign, 2016).